Hall effects on peristaltic flow of couple stress fluid in a vertical asymmetric channel

IOP Conf. Series: Materials Science and Engineering **263** (2017) 062021 doi:10.1088/1757-899X/263/6/062021

Hall effects on peristaltic flow of couple stress fluid in a vertical asymmetric channel

P Maninaga Kumar [1], A Kavitha [1] and R Saravana[2]
[1] Department of Mathematics, School of Advanced Sciences, VIT University, Vellore, Tamil Nadu – 632014, India
[2] Department of Mathematics, MITS, Madanapalli, Andhra Pradesh, India

E-mail: kavitha@vit.ac.in

Abstract: The influence of Hall effect on peristaltic transport of a couple stress fluid in a vertical asymmetric channel is examined. The problem is solved under the assumptions of low Reynolds number and long wavelength. The velocity, temperature and concentration are obtained by using analytical solutions. Effect of Hall parameter, couple stress fluid parameter, Froude number, Hartmann number and the phase difference on the pumping characteristics, temperature and concentration are discussed graphically.

1. Introduction

The phenomenon of a peristaltic transport of fluid is appears in a number of physiological and engineering applications like movement of chyme in the gastrointestinal tract, urine transport from kidney to bladder, mixing and transporting the contents of the gastrointestinal passage, vasomotion of small blood vessels such as arterioles, movement of ovum in the female fallopian tube etc. Latham [1] and Shapiro et al. [2] were one of the first researchers on peristaltic flow movement. After that by using analytical, numerical and experimental methods, analysis of peristaltic flows of viscous fluids are studied. Later peristaltic flows effects on magneto hydrodynamic fluids are reviewed.

The effect of applied magnetic field and heat transfer in the peristaltic flows are also analyzed in view of MHD character of blood, magneto hydrodynamic power generators, method of hemodialysis, oxygenation and hyperthermia. A few of the researchers who further studied in this field are [3, 4, 8, 12]. Prabakaran et al. [5] Concentrated on the magneto hydrodynamic peristaltic transport of a Jeffrey fluid in a permeable channel with the impact of compliant walls, heat and mass transfer under the various assumptions of long wavelength and low Reynolds number. Saravana et al. [6] has made discussions on the heat and mass exchange on the unstable visco-versatile second order Rivlin-Erickson liquid past an infinite vertical plate in the presence of constant mass flux Vajravelu et al. [7] The impact of velocity slip, temperature and concentration conditions on the MHD peristaltic flow of a Carreau liquid in a non-uniform channel with warmth and mass exchange is explored. Hari Prabakaran et al. [10] The Peristaltic stream of a fourth grade liquid between two permeable walls with suction and infusion is examined. Saravana et al. [11] Concentrate the Peristaltic transport of MHD Jeffrey liquid in a non-uniform permeable channel with the impact of slip, divider properties and warmth exchange under the suspicions of long wavelength and low Reynolds number.

Stokes [14] presented the theory of couple stress fluids in which the size-dependent effect in the presence of couple stresses; body couples and non-symmetric stress tensor are found. Cowin [15], Beg et al. [16] and Ali et al. [17] stressed the importance of couple stress effects in studies related to

physiological and some other fluids. The Hall effects in peristaltic movement of Maxwell fluid are done by Hayat et al. [18]. Srinivas et al. [19] studied the problem of peristaltic flow of a Newtonian fluid with heat transfer in a vertical asymmetric channel through porous medium. Nadeem et al. [20] discussed about the influence of heat and mass transfer on the peristaltic flow of a Johnson Segalman fluid with induced magnetic field. Kavitha et al. [21] reviewed the peristaltic flow of a micropolar fluid in a vertical channel with long wavelength approximation. Vajravelu et al. [22] investigated the peristaltic flow of a Jeffrey fluid in a vertical porous stratum with heat transfer. Rami Reddy et al. [23] explored the peristaltic motion of a viscous conducting fluid through a porous medium in an asymmetric vertical channel by using Lubrication approach. Gad [24] studied the peristaltic flow of a particle-fluid in regards to Hall current. Abo-Eldahab et al [25] discussed the Hall current in peristaltic flow of viscous fluid in a vertical asymmetric channel. Hayat et al. [26] discussed the peristaltic flow of couple stress fluid in an inclined asymmetric channel. The effects of Hall current, heat and mass transfer in the presence of inclined magnetic fluid are also reviewed.

In this existing paper, we discussed about the Hall effects on peristaltic flow of couple stress fluid in a vertical asymmetric channel. The velocity, pressure gradient, temperature and concentration profiles are obtained and the results are discussed graphically.

2 .Mathematical formulation

Let us assume that the two-dimensional peristaltic flow of couple stress fluid in a vertical asymmetric channel. The right and left vertical walls of channel are separated by a distance $d_1 + d_2$, the temperature maintained at right and left vertical walls are T_0 and T_1, respectively. The concentration field associated to right and left vertical walls are taken as C_0 and C_1, respectively.

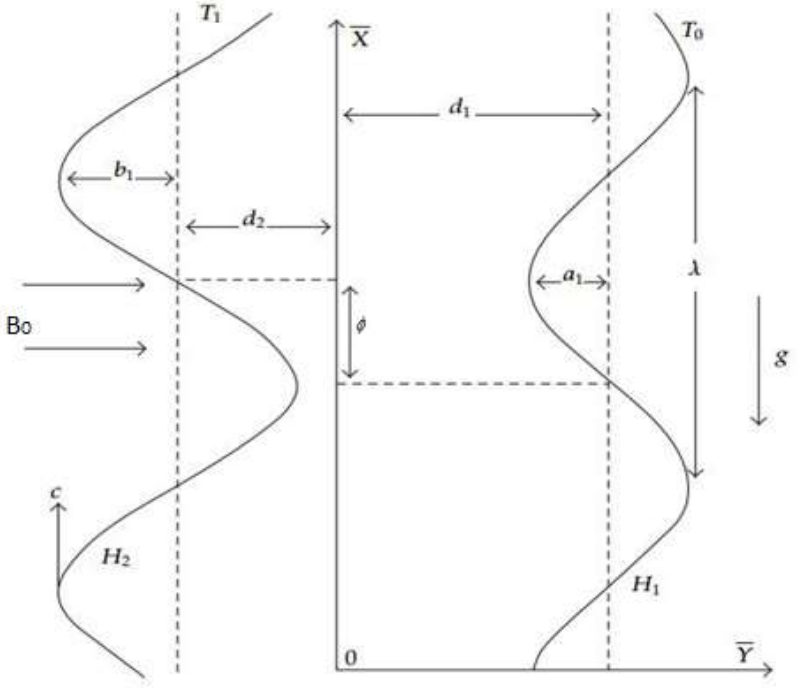

Figure 1. Physical model

The basic governing equations are:

$$\frac{\partial \bar{U}}{\partial \bar{X}} + \frac{\partial \bar{V}}{\partial \bar{Y}} = 0, \tag{1}$$

$$\rho\left(\frac{\partial}{\partial t} + \bar{U}\frac{\partial}{\partial \bar{X}} + \bar{V}\frac{\partial}{\partial \bar{Y}}\right)\bar{U} = -\frac{\partial \bar{P}}{\partial \bar{X}} + \mu\left(\frac{\partial^2 \bar{U}}{\partial \bar{X}^2} + \frac{\partial^2 \bar{U}}{\partial \bar{Y}^2}\right) - \eta^*\left(\frac{\partial^4 \bar{U}}{\partial \bar{X}^2} + 2\frac{\partial^4 \bar{U}}{\partial \bar{X}^2 \partial \bar{Y}^2} + \frac{\partial^4 \bar{U}}{\partial \bar{Y}^4}\right) - \frac{\sigma^* B_0^2}{1+m^2}(\bar{U} + m\bar{V}) + g\rho, \tag{2}$$

$$\rho\left(\frac{\partial}{\partial t} + \bar{U}\frac{\partial}{\partial \bar{X}} + \bar{V}\frac{\partial}{\partial \bar{Y}}\right)\bar{V} = -\frac{\partial \bar{P}}{\partial \bar{Y}} + \mu\left(\frac{\partial^2 \bar{V}}{\partial \bar{X}^2} + \frac{\partial^2 \bar{V}}{\partial \bar{Y}^2}\right) - \eta^*\left(\frac{\partial^4 \bar{V}}{\partial \bar{X}^2} + 2\frac{\partial^4 \bar{V}}{\partial \bar{X}^2 \partial \bar{Y}^2} + \frac{\partial^4 \bar{V}}{\partial \bar{Y}^4}\right) + \frac{\sigma^* B_0^2}{1+m^2}(m\bar{U} - \bar{V}) + g\rho, \tag{3}$$

$$\rho\xi\left(\frac{\partial}{\partial \bar{t}} + \bar{U}\frac{\partial}{\partial \bar{X}} + \bar{V}\frac{\partial}{\partial \bar{Y}}\right)T = k\left(\frac{\partial^2 T}{\partial \bar{X}^2} + \frac{\partial^2 T}{\partial \bar{Y}^2}\right) + \mu\left[2\left(\frac{\partial \bar{U}}{\partial \bar{X}}\right)^2 + 2\left(\frac{\partial \bar{V}}{\partial \bar{Y}}\right)^2 + \left(\frac{\partial \bar{U}}{\partial \bar{Y}} + \frac{\partial \bar{V}}{\partial \bar{X}}\right)^2\right] + \eta^*\left[\left(\frac{\partial^2 \bar{V}}{\partial \bar{X}^2} + \frac{\partial^2 \bar{V}}{\partial \bar{Y}^2}\right)^2 + \left(\frac{\partial^2 \bar{U}}{\partial \bar{X}^2} + \frac{\partial^2 \bar{U}}{\partial \bar{Y}^2}\right)^2\right] + \frac{\rho D K_T}{c_s}\left(\frac{\partial^2 C}{\partial \bar{X}^2} + \frac{\partial^2 C}{\partial \bar{Y}^2}\right), \tag{4}$$

$$\left(\frac{\partial}{\partial \bar{t}} + \bar{U}\frac{\partial}{\partial \bar{X}} + \bar{V}\frac{\partial}{\partial \bar{Y}}\right)C = D\left(\frac{\partial^2 C}{\partial \bar{X}^2} + \frac{\partial^2 C}{\partial \bar{Y}^2}\right) + \frac{DK_T}{T_m}\left(\frac{\partial^2 T}{\partial \bar{X}^2} + \frac{\partial^2 T}{\partial \bar{Y}^2}\right), \tag{5}$$

The geometry of the channel walls is given by

$$\bar{Y} = \bar{h}_1 = d_1 + a_1 \sin\left[\frac{2\pi}{\lambda}\left(\bar{X} - c\bar{t}\right)\right], \tag{6}$$

$$\bar{Y} = \bar{h}_2 = -d_2 + a_2 \sin\left[\frac{2\pi}{\lambda}\left(\bar{X} - c\bar{t}\right) + \phi\right], \tag{7}$$

. In Eqs. (1) - (7), where $\bar{P}$ represents the pressure, C - fluid concentration, T - fluid temperature, κ - thermal conductivity, ξ - specific heat at constant pressure, T_m - mean temperature of the medium, D - coefficient of mass diffusivity, ρ - fluid density, K_T - thermal-diffusion ratio, $\bar{U}$ - longitudinal velocity component, $\bar{V}$ - transverse velocity component and wavelength respectively. Here, η^* - couple stress fluid parameter, c_s - concentration susceptibility, $a_i (i = 1,2)$ - wave amplitudes of the right and left vertical walls, $\bar{t}$ - time, B_0 - applied magnetic field, σ^* - electrical conductivity, $\bar{U}, \bar{V}$ - velocity components in fixed frame, $m\left(= \sigma^* B_0 / en\right)$ - Hall parameter, n - number density of electrons, e - electric charge . ϕ - phase difference varied between $0 \le \phi \le \pi$.

$$a_1^2 + a_2^2 + 2a_1a_2\cos\phi \le (d_1 + d_2)^2. \tag{8}$$

Defining the transformations

$$\begin{aligned} &\bar{x} = \bar{X} - c\bar{t}, \quad \bar{y} = \bar{Y}, \quad \bar{u}(\bar{x},\bar{y}) = \bar{U}(\bar{X},\bar{Y},\bar{t}) - c, \\ &\bar{v}(\bar{x},\bar{y}) = \bar{V}(\bar{X},\bar{Y},\bar{t}), \quad \bar{p}(\bar{x},\bar{y}) = \bar{P}(\bar{X},\bar{Y},\bar{t}), \end{aligned} \tag{9}$$

The equations in wave frame become

$$\frac{\partial \bar{u}}{\partial \bar{x}} + \frac{\partial \bar{v}}{\partial \bar{y}} = 0, \tag{10}$$

$$\begin{aligned} \rho\left(\bar{u}\frac{\partial}{\partial \bar{x}} + \bar{v}\frac{\partial}{\partial \bar{y}}\right)\bar{u} = &-\frac{\partial \bar{p}}{\partial \bar{x}} + \mu\left(\frac{\partial^2 \bar{u}}{\partial \bar{x}^2} + \frac{\partial^2 \bar{u}}{\partial \bar{y}^2}\right) - \eta^*\left(\frac{\partial^4 \bar{u}}{\partial \bar{x}^4} + 2\frac{\partial^4 \bar{u}}{\partial \bar{x}^2 \partial \bar{y}^2} + \frac{\partial^4 \bar{u}}{\partial \bar{y}^4}\right) \\ &- \frac{\sigma^* B_0^2}{1+m^2}(\bar{u} + m\bar{v}) + g\rho, \end{aligned} \tag{11}$$

$$\begin{aligned} \rho\left(\bar{u}\frac{\partial}{\partial \bar{x}} + \bar{v}\frac{\partial}{\partial \bar{y}}\right)\bar{v} = &-\frac{\partial \bar{p}}{\partial \bar{y}} + \mu\left(\frac{\partial^2 \bar{v}}{\partial \bar{x}^2} + \frac{\partial^2 \bar{v}}{\partial \bar{y}^2}\right) - \eta^*\left(\frac{\partial^4 \bar{v}}{\partial \bar{x}^4} + 2\frac{\partial^4 \bar{v}}{\partial \bar{x}^2 \partial \bar{y}^2} + \frac{\partial^4 \bar{v}}{\partial \bar{y}^4}\right) \\ &+ \frac{\sigma^* B_0^2}{1+m^2}(m\bar{u} - \bar{v}) - g\rho, \end{aligned} \tag{12}$$

$$\begin{aligned} \rho\xi\left(\bar{u}\frac{\partial}{\partial \bar{x}} + \bar{v}\frac{\partial}{\partial \bar{y}}\right)T = &\, k\left(\frac{\partial^2 T}{\partial \bar{x}^2} + \frac{\partial^2 T}{\partial \bar{y}^2}\right) + \mu\left[2\left(\frac{\partial \bar{u}}{\partial \bar{x}}\right)^2 + 2\left(\frac{\partial \bar{u}}{\partial \bar{y}}\right)^2 + \left(\frac{\partial \bar{u}}{\partial \bar{y}} + \frac{\partial \bar{v}}{\partial \bar{x}}\right)^2\right] \\ &+ \eta^*\left[\left(\frac{\partial^2 \bar{v}}{\partial \bar{x}^2} + \frac{\partial^2 \bar{v}}{\partial \bar{y}^2}\right)^2 + \left(\frac{\partial^2 \bar{u}}{\partial \bar{x}^2} + \frac{\partial^2 \bar{u}}{\partial \bar{y}^2}\right)^2\right] + \frac{\rho D K_T}{c_s}\left(\frac{\partial^2 C}{\partial \bar{x}^2} + \frac{\partial^2 C}{\partial \bar{y}^2}\right), \end{aligned} \tag{13}$$

$$\left(\bar{u}\frac{\partial}{\partial \bar{x}} + v\frac{\partial}{\partial \bar{y}}\right)C = D\left(\frac{\partial^2 C}{\partial \bar{x}^2} + \frac{\partial^2 C}{\partial \bar{y}^2}\right) + \frac{DK_T}{T_m}\left(\frac{\partial^2 T}{\partial \bar{x}^2} + \frac{\partial^2 T}{\partial \bar{y}^2}\right) \tag{14}$$

The non-dimensional quantities

$$\begin{aligned} &x = \frac{\bar{x}}{\lambda},\ y = \frac{\bar{y}}{d_1},\ u = \frac{\bar{u}}{c},\ v = \frac{\bar{v}}{c\delta},\ p = \frac{d_1^2}{c\mu\lambda}\bar{p},\ h_1 = \frac{h_1}{d_1},\ h_2 = \frac{h_2}{d_1} \\ &\delta = \frac{d_1}{\lambda},\ \eta = \frac{\eta^*}{\mu d_1^2},\ R_e = \frac{\rho c d_1}{\mu},\ Fr = \frac{c^2}{g d_1},\ k = \frac{k_0 c}{\mu d_1},\ \Phi = \frac{d_1^2}{\mu c^2}\overline{\Phi} \\ &\gamma = \frac{T - T_0}{T_1 - T_0},\ Ec = \frac{c^2}{\xi(T_1 - T_0)},\ \mathrm{Pr} = \frac{\xi\mu}{k},\ \varphi = \frac{C - C_0}{C_1 - C_0},\ Sc = \frac{\mu}{\rho D}, \\ &Sr = \frac{\rho D K_T(C_1 - C_0)}{\mu T_m(T_1 - T_0)},\ Du = \frac{\rho D K_T(C_1 - C_0)}{\mu\xi c_s(T_1 - T_0)},\ M^2 = \frac{\sigma^* B_0^2 d_1^2}{\mu},\ Br = \mathrm{Pr}\,Ec. \end{aligned} \tag{15}$$

Eqs. (10) – (14) take the forms

$$\frac{\partial u}{\partial x}+\frac{\partial v}{\partial y}=0, \tag{16}$$

$$\delta \mathrm{Re}\left(u\frac{\partial}{\partial x}+v\frac{\partial}{\partial y}\right)u=-\frac{\partial p}{\partial x}+\delta^2\frac{\partial^2 u}{\partial x^2}+\frac{\partial^2 u}{\partial y^2}-\eta\left(\delta^4\frac{\partial^4 u}{\partial x^4}+2\delta^2\frac{\partial^4 u}{\partial x^2\partial y^2}+\frac{\partial^4 u}{\partial y^4}\right) -\frac{M^2}{1+m^2}(u+\delta m v)+\frac{\mathrm{Re}}{Fr}, \tag{17}$$

$$\delta^3 \mathrm{Re}\left(u\frac{\partial}{\partial x}+v\frac{\partial}{\partial y}\right)v=-\frac{\partial p}{\partial y}+\delta^2\left(\delta^2\frac{\partial^2 v}{\partial x^2}+\frac{\partial^2 v}{\partial y^2}\right)-\eta\delta^2\left(\delta^4\frac{\partial^4 v}{\partial x^4}+2\delta^2\frac{\partial^4 v}{\partial x^2\partial y^2}+\frac{\partial^4 v}{\partial y^4}\right) +\frac{M^2}{1+m^2}(mu-\delta v)-\delta\frac{\mathrm{Re}}{Fr}, \tag{18}$$

$$\delta \mathrm{Re}\,\mathrm{Pr}\left(u\frac{\partial}{\partial x}+v\frac{\partial}{\partial y}\right)\gamma=\delta^2\frac{\partial^2\gamma}{\partial x^2}+\frac{\partial^2\gamma}{\partial y^2}+Br\left[2\delta^2\left(\frac{\partial u}{\partial x}\right)^2+2\delta^2\left(\frac{\partial v}{\partial y}\right)^2\times\left(\frac{\partial u}{\partial y}+\delta^2\frac{\partial v}{\partial x}\right)^2\right] +\eta Br\left[\delta^2\left(\delta^2\frac{\partial^2 v}{\partial x^2}+\frac{\partial^2 v}{\partial y^2}\right)^2+\left(\delta^2\frac{\partial^2 u}{\partial x^2}+\frac{\partial^2 u}{\partial y^2}\right)^2\right] +\mathrm{Pr}\,Du\left(\delta^2\frac{\partial^2\varphi}{\partial x^2}+\frac{\partial^2\varphi}{\partial y^2}\right), \tag{19}$$

$$\delta \mathrm{Re}\left(u\frac{\partial}{\partial x}+v\frac{\partial}{\partial y}\right)\varphi=\frac{1}{Sc}\left(\delta^2\frac{\partial^2\varphi}{\partial x^2}+\frac{\partial^2\varphi}{\partial y^2}\right)+Sr\left(\delta^2\frac{\partial^2\gamma}{\partial x^2}+\frac{\partial^2\gamma}{\partial y^2}\right), \tag{20}$$

where Re represents the Reynolds number, Fr - Froude number, Pr - Prandtl number. Br - Brinkman number, Du - Dufour number, Sc - Schmidt number and Sr- Soret number.

The assumptions of long wave length $(\delta << 1)$

Eqs. (17) – (20) give

$$-\frac{\partial p}{\partial x}+\frac{\partial^2 u}{\partial y^2}-\eta\frac{\partial^4 u}{\partial y^4}-\frac{M^2}{1+m^2}u+\frac{\mathrm{Re}}{Fr}=0, \tag{21}$$

$$\frac{\partial^2\gamma}{\partial y^2}+Br\left(\frac{\partial u}{\partial y}\right)^2+\eta Br\left(\frac{\partial^2 u}{\partial y^2}\right)^2+\mathrm{Pr}\,Du\frac{\partial^2\varphi}{\partial y^2}=0, \tag{22}$$

$$\frac{\partial^2\varphi}{\partial y^2}+ScSr\frac{\partial^2\gamma}{\partial y^2}=0, \tag{23}$$

Eq.s (21) –(23) satisfies the incompressibility condition and Eq.(20) shows that $p\neq p(y)$.

Boundary conditions and vertical wall properties $h_1(x)$ and $h_2(x)$ in the lacking dimension form are

$$u=-1,\quad \frac{\partial^2 u}{\partial y^2}=0,\quad \gamma=0,\quad \varphi=0,\qquad at\ \ y=h_1=1+a\sin(2\pi x), \tag{24}$$

$$u=-1,\quad \frac{\partial^2 u}{\partial y^2}=0,\quad \gamma=1,\quad \varphi=1,\qquad at\ \ y=h_2=-d-b\sin(2\pi x+\phi), \tag{25}$$

where $a=a_1/d_1,\ \ b=a_2/d_1\ and\ d=d_2/d_1$ satisfy the condition

$$a^2+b^2+2ab\cos\phi\le(1+d)^2. \tag{26}$$

The lacking dimension average flux F in the wave frame is

$$F=\int_{h_2}^{h_1} u\,dy. \tag{27}$$

The relation of average flux in the laboratory frame σ is

$$\sigma=F+1+d. \tag{28}$$

The pressure rise per wavelength Δp_λ is as follows

$$\Delta p_\lambda=\int_0^1\left(\frac{dp}{dx}\right)dx. \tag{29}$$

2.1 Solutions of the problem

By solving Eq. (21), we get

$$u(y)=C_1e^{yM_1}+C_2e^{-yM_1}+C_3e^{yM_2}+C_4e^{-yM_2}-\frac{H}{z}, \tag{30}$$

$$\text{where}\ \ k=\frac{M^2}{1+m^2},\qquad H=-\frac{\mathrm{Re}}{Fr}+\frac{dp}{dx}. \tag{31}$$

By using Eqs. (27), (30) and (31), we can find $\frac{dp}{dx}$.

To find the solution of $\gamma(y)$, by putting Eqs. (30), (31) and (23) into Eq. (22).

$$\gamma = C_5 + C_6 y + \frac{Br}{-1+\Pr DuScSr}\left[\begin{array}{l}\frac{1}{4}C_1^2\left(1+\eta M_1^2\right)e^{2M_1 y}+\frac{1}{4}C_2^2\left(1+\eta M_1^2\right)e^{-2M_1 y}+\frac{1}{4}C_3^2\left(1+\eta M_2^2\right)e^{2M_2 y}\\ +\frac{1}{4}C_4^2\left(1+\eta M_2^2\right)e^{-2M_1 y}+2M_1M_2C_1C_3\left(-1+\eta M_1M_2\right)\frac{e^{(M_1+M_2)y}}{\left(M_1+M_2\right)^2}\\ +2M_1M_2C_1C_4\left(-1+\eta M_1M_2\right)\frac{e^{(M_1-M_2)y}}{\left(M_1-M_2\right)^2}\\ +2M_1M_2C_2C_3\left(-1+\eta M_1M_2\right)\frac{e^{-(M_1-M_2)y}}{\left(M_1-M_2\right)^2}\\ +2M_1M_2C_2C_4\left(1+\eta M_1M_2\right)\frac{e^{-(M_1+M_2)y}}{\left(M_1+M_2\right)^2}\\ +M_1^2C_1C_2\left(-1+\eta M_1^2\right)y^2+M_2^2C_3C_4\left(-1+\eta M_2^2\right)y^2\end{array}\right] \tag{32}$$

By solving Eq. (23), we get the solution of φ

$$\varphi = C_7 + C_8 y - \frac{ScSrBr}{-1+\Pr DuScSr}\left[\begin{array}{l}\frac{1}{4}C_1^2\left(1+\eta M_1^2\right)e^{2M_1 y}+\frac{1}{4}C_2^2\left(1+\eta M_1^2\right)e^{-2M_1 y}+\frac{1}{4}C_3^2\left(1+\eta M_2^2\right)e^{2M_2 y}\\ +\frac{1}{4}C_4^2\left(1+\eta M_2^2\right)e^{-2M_1 y}+2M_1M_2C_1C_3\left(1+\eta M_1M_2\right)\frac{e^{(M_1+M_2)y}}{\left(M_1+M_2\right)^2}\\ +2M_1M_2C_1C_4\left(-1+\eta M_1M_2\right)\frac{e^{(M_1-M_2)y}}{\left(M_1-M_2\right)^2}\\ +2M_1M_2C_2C_3\left(1+\eta M_1M_2\right)\frac{e^{-(M_1-M_2)y}}{\left(M_1-M_2\right)^2}\\ +2M_1M_2C_2C_4\left(1+\eta M_1M_2\right)\frac{e^{-(M_1+M_2)y}}{\left(M_1+M_2\right)^2}\\ +M_1^2C_1C_2\left(-1+\eta M_1^2\right)y^2+M_2^2C_3C_4\left(-1+\eta M_2^2\right)y^2\end{array}\right] \tag{33}$$

$$\text{where } M_1 = \sqrt{-\frac{-1+\sqrt{1-4k\eta}}{2\eta}} \text{ and } M_2 = \sqrt{\frac{-1+\sqrt{1-4k\eta}}{2\eta}} \tag{34}$$

Using the boundary condition and the Eqs. (30), (32) and (33), calculated constants $C_i\left(i=1-8\right)$

3. Results and Discussion

3.1 Pumping characteristics

Here we discussed about the longitudinal pressure gradient dp/dx and pressure rise per wavelength Δp_λ for different flow parameters concerned in the current problem. Here we calculated eq. (31) numerically by using "Mathematica". Figure 2 is plotted between dp/dx for various values of couple

stress parameter η and x. "It is realized that pressure gradient increases in the narrow part of the channel while it decreases near the wider part of the channel. It is interesting to note that resistance or assistance from dp/dx for a non-Newtonian fluid $(\eta \neq 0)$ is higher than that of a Newtonian fluid $(\eta \to 0)$" . Figure 3 depicts the impact of Hall parameter m on dp/dx. It shows that dp/dx decreases in the channel where it is narrow and it increases in the channel where it is wider. Figure 4 represents that Hartmann number M increase with increase of dp/dx in narrow part of the channel while dp/dx decreases at the wider part of the channel. In Figure 5, we deduced that various values of Fr, dp/dx decreases the entire channel. Figure 6 depicts that dp/dx is initially increases and finally decreases with the increases of ϕ.

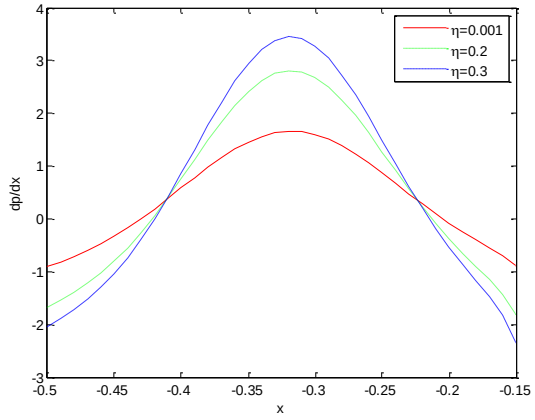

Figure 2. Plot of pressure gradient dp/dx for various values of η with $a = 0.6$, b=0.7, d=1.5, R = 0.5, $\phi = \pi/4$, m=0.03, Fr=1.2, $\theta = \pi/3$ and M=4.

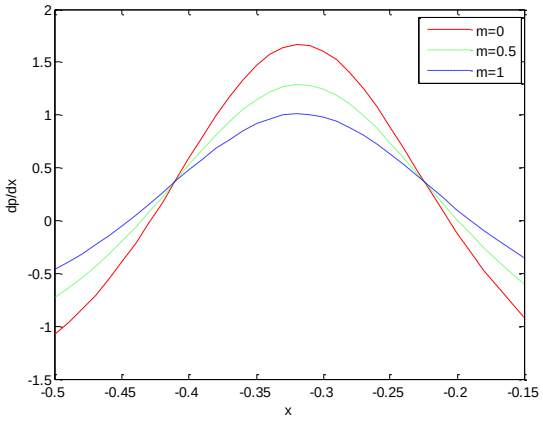

Figure 3. Plot of pressure gradient dp/dx for various values of m with $a = 0.6$, b=0.7, d=1.5, R = 0.5, $\phi = \pi/4$, $\eta = 0.1$, Fr=1.2, $\theta = \pi/3$ and M=4.

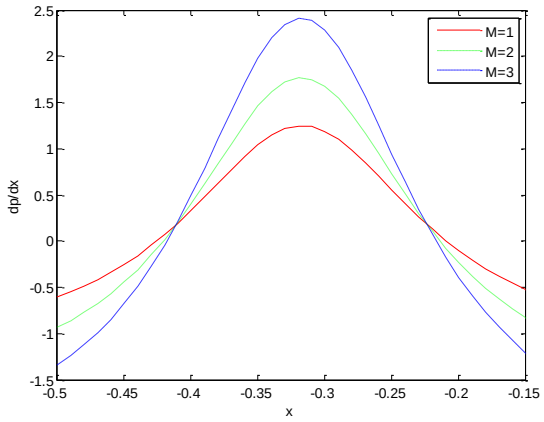

Figure 4. Plot of pressure gradient dp/dx for various values of M with $a=0.6$, b=0.7, d=1.5, R = 0.5, $\phi=\pi/4$, $\eta=0.1$, Fr=1.2, $\theta=\pi/3$ and m=0.03.

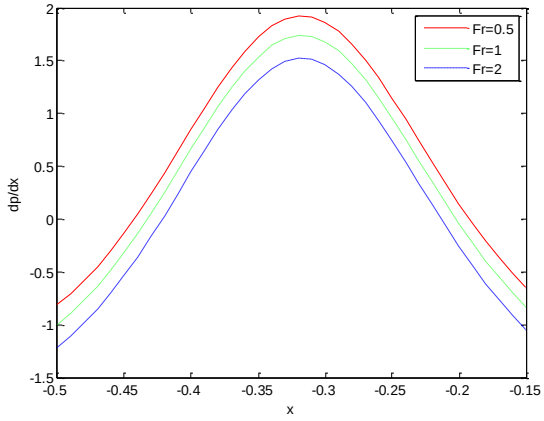

Figure 5. Plot of pressure gradient dp/dx for various values of Fr with $a=0.6$, b=0.7, d=1.5, R = 0.5, $\phi=\pi/4$, $\eta=0.1$, M=4, $\theta=\pi/3$ and m=0.03.

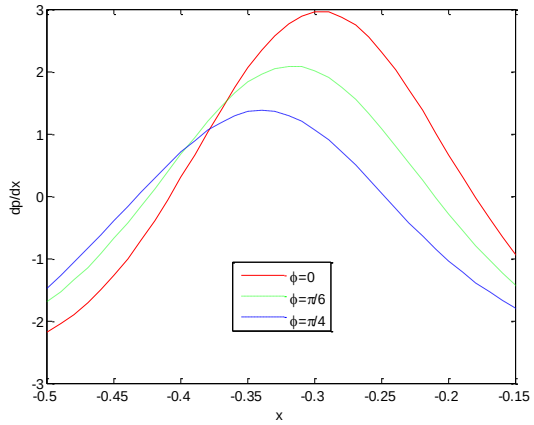

Figure 6. Plot of pressure gradient dp/dx for various values of ϕ with $a=0.6$, b=0.7, d=1.5, R = 0.5, Fr=1.2, $\eta=0.1$, M=4, $\theta=\pi/3$ and m=0.03.

Figures 7-11 represents the different values of the pressure rise per wavelength Δp_λ against average flux σ. In Figure7, noted that in peristaltic pumping region $(\Delta p_\lambda > 0, \sigma > 0)$ the pressure rise increases where as it decreases in the copumping region $(\Delta p_\lambda < 0,\ \sigma > 0)$ with couple stress parameter η increase. "Figure 8 represents the pressure rise Δp_λ when the flow is subcritical $(Fr < 1)$ the pressure rise has greater effect than the critical flow $(Fr = 1)$ and supercritical flow $(Fr > 1)$ which means that the flow becomes slow by increasing Froude number Fr and so pressure rise Δp_λ decreases". In Figure 9, the pressure rise Δp_λ increases in the peristaltic pimping region $(\Delta p_\lambda > 0, \sigma > 0)$ and it decreases in the copumping region $(\Delta p_\lambda < 0, \sigma > 0)$ with the increase of Hartman number M. Figure 10 shows that the pressure rise decreases in the retrograde $(\Delta p_\lambda > 0, \sigma < 0)$ region and it increases in the co pumping region $(\Delta p_\lambda < 0, \sigma > 0)$ with the increases of Hall parameter m. Figure 11 reveals that Δp_λ decreases in the peristaltic pumping region $(\Delta p_\lambda > 0, \sigma > 0)$ and increases in copumping region $(\Delta p_\lambda < 0, \sigma > 0)$ while it decreases in the retrograde $(\Delta p_\lambda > 0, \sigma > 0)$ region with an increase in phase difference ϕ.

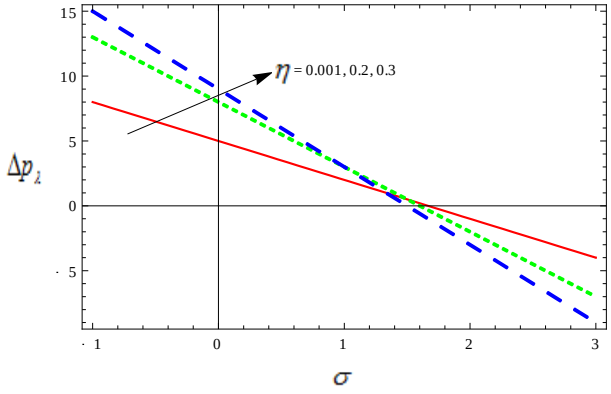

Figure 7. Plot of pressure rise Δp_λ for various values of η with $a = 0.7$, b=1.2, d=2, R=0.5, Fr=1.2, $\phi = \pi/4$, m= 0.03, M=4 and $\theta = \pi/3$.

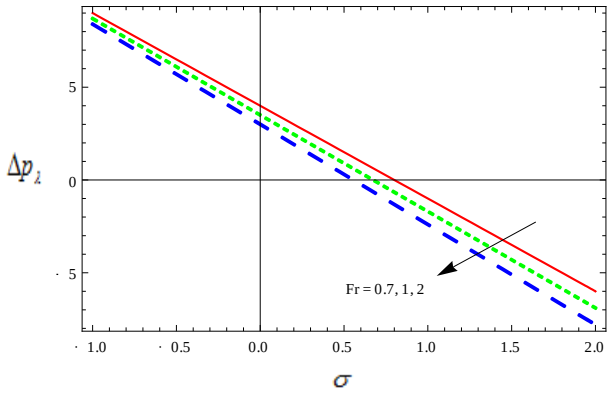

Figure 8. Plot of pressure rise Δp_λ for various values of Fr with $a = 0.7$, b=1.2, d=2, R=0.5, $\eta = 0.1$, $\phi = \pi/4$, m= 0.03, M=4 and $\theta = \pi/3$.

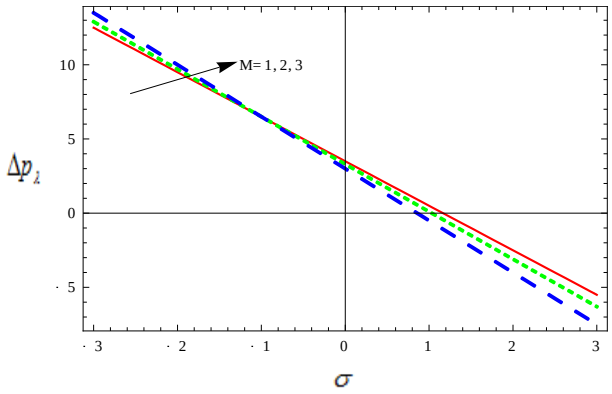

Figure 9. Plot of pressure rise Δp_λ for various values of M with $a=0.7$, b=1.2, d=2, R=0.5, $\eta=0.1$, $\phi=\pi/4$, m= 0.03, Fr=1.2 and $\theta=\pi/3$.

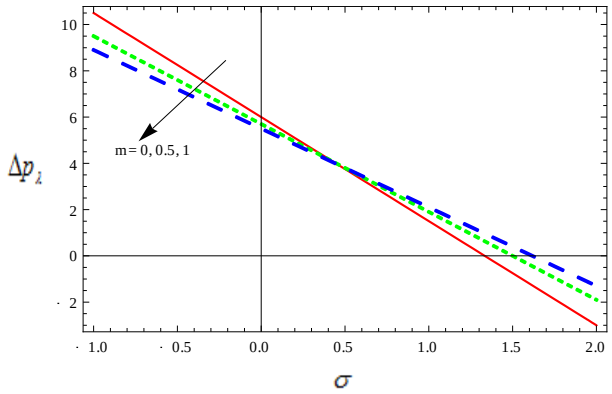

Figure 10. Plot of pressure rise Δp_λ for various values of m with $a=0.7$, b=1.2, d=2, R=0.5, $\eta=0.1$, $\phi=\pi/4$, M= 4, Fr=1.2 and $\theta=\pi/3$.

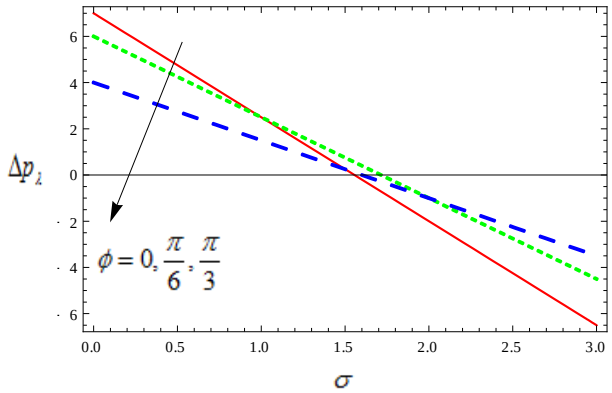

Figure 11. Plot of pressure rise Δp_λ for various values of ϕ with $a=0.7$, b=1.2, d=2, R=0.5, $\eta=0.1$, $\theta=\pi/3$, M= 4, Fr=1.2 and m=0.03.

3.2 *Velocity behavior*

The impact of several physical parameters on the velocity profile $u(y)$ is analyzed. Figure 12 depicts that magnitude of the velocity profile $u(y)$ decreases with the increases of couple stress parameter η. It is noted that form Figure 13, "for subcritical flow $(Fr<1)$ the velocity profile $u(y)$ has

strengthened than that for critical $(Fr=1)$ and supercritical $(Fr>1)$ flow cases". The velocity profile $u(y)$ is quite opposite to Froude number Fr. Figures 14 and 15 reveal that decreases $u(y)$ while increase of Hartmann number M and Hall parameter m.

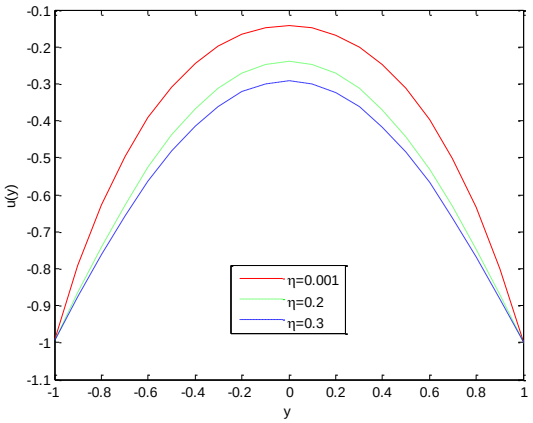

Figure 12. Plot of velocity field $u(y)$ for various values of η with $a=0.6$, b=0.7, d=1.5, R=2,Fr=1.2, $\sigma=1$, M=4,m=0.03,x=-0.5, $\phi=\pi/4$, $\theta=\pi/3$ and $dp/dx=1$.

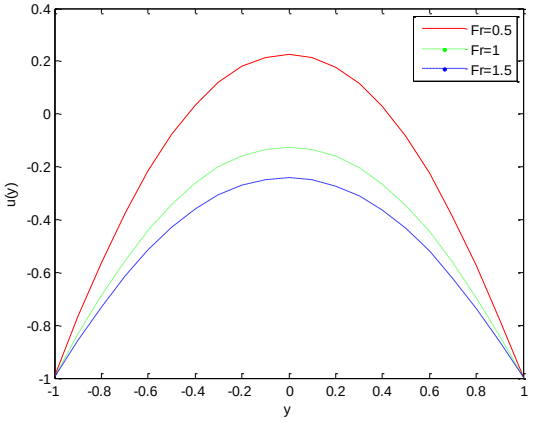

Figure 13. Plot of velocity field $u(y)$ for various values of Fr with $a=0.6$, b=0.7, d=1.5, R=2, $\eta=0.1$, $\sigma=1$, M=4,m=0.03,x=-0.5, $\phi=\pi/4$, $\theta=\pi/3$ and $dp/dx=1$.

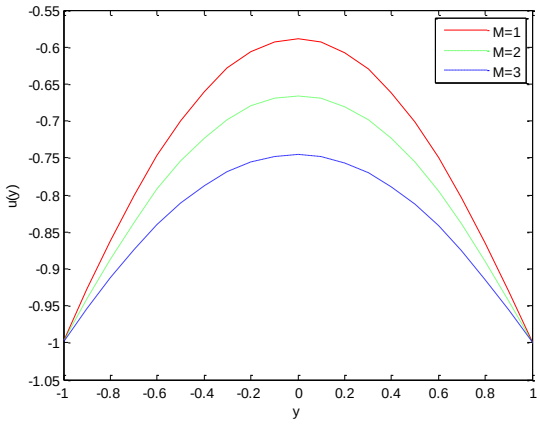

Figure 14. Plot of velocity field $u(y)$ for various values of M with $a=0.6$, b=0.7, d=1.5, R=2, $\eta=0.1$, $\sigma=1$, Fr=1.2,m=0.03,x=-0.5, $\phi=\pi/4$, $\theta=\pi/3$ and $dp/dx=1$.

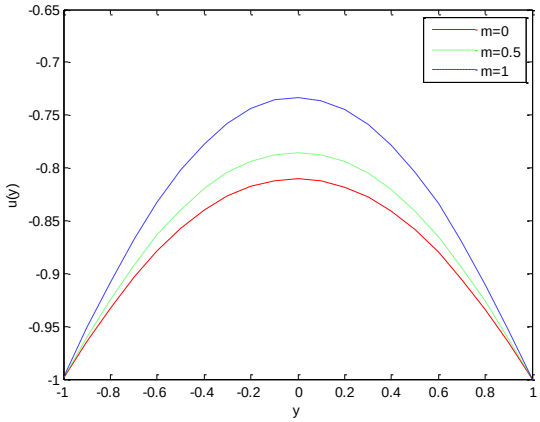

Figure 15. Plot of velocity field $u(y)$ for various values of m with $a=0.6$, b=0.7, d=1.5, R=2, $\eta=0.1$, $\sigma=1$, Fr=1.2,M=4,x=-0.5, $\phi=\pi/4$, $\theta=\pi/3$ and $dp/dx=1$.

3.3 Temperature profile.

Figures 16-19 shows that the differences of the temperature profile $\gamma(y)$ for various values of parameters of interest. In Figure 16, we observed that $\gamma(y)$decreases as couple stress parameter η increases. As per Figure 17, the temperature profile $\gamma(y)$ and Hartmann number M are in inversely proportional. Figure 18 represents that the $\gamma(y)$ increases with the increases of Hall parameter m. Figure 19 illustrates, "the temperature profile $\gamma(y)$ has greater effects for supercritical flow $(Fr>1)$ and critical flow $(Fr=1)$ than subcritical flow$(Fr<1)$". Thus $\gamma(y)$ is directly proportional to Froude number Fr.

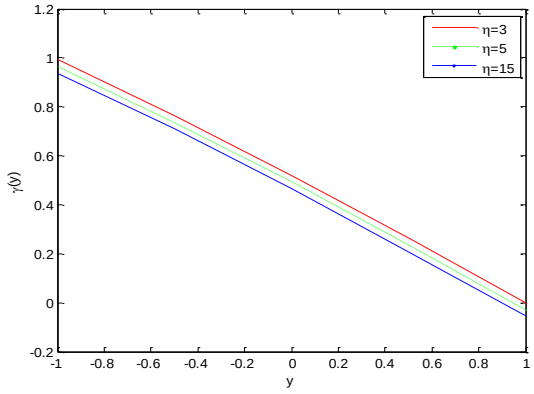

Figure 16. Plot of temperature profile $\gamma(y)$ for various values of η with $a=0.6$, b=0.7, d=1.5, R=0.5, M=4, Fr=1.2, m=0.03, x=-0.5, Du=0.1, Sc=0.5,Br=Pr=2, Sr=0.6 $\sigma=1,\phi=\pi/4,\theta=\pi/3$ and $dp/dx=1$.

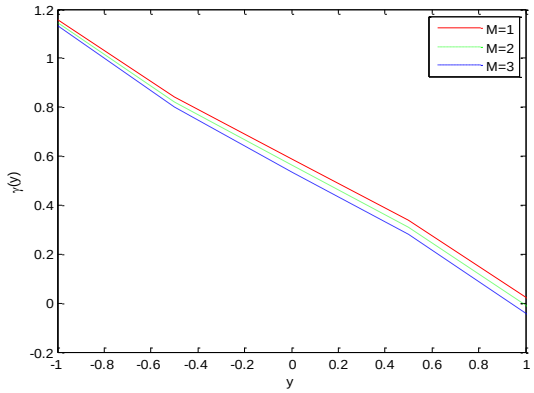

Figure 17. Plot of temperature profile $\gamma(y)$ for various values of M with $a=0.6$, b=0.7, d=1.5, R=0.5, $\eta=0.1$,Fr=1.2, m=0.03, x=-0.5, Du=0.1, Sc=0.5,Br=Pr=2, Sr=0.6 $\sigma=1,\phi=\pi/4,\theta=\pi/3$ and $dp/dx=1$

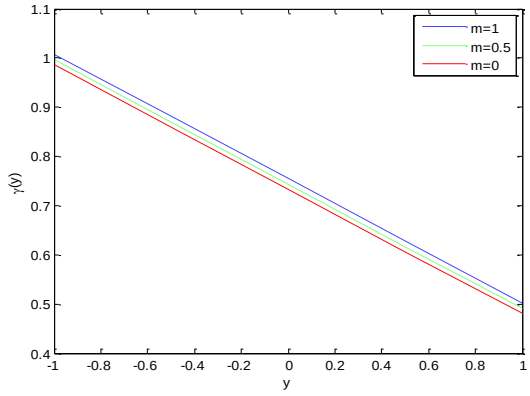

.

Figure 18. Plot of temperature profile $\gamma(y)$ for various values of m with $a=0.6$, b=0.7, d=1.5, R=0.5, $\eta=0.1$,Fr=1.2, $\theta=\pi/3$, x=-0.5, Du=0.1, Sc=0.5,Br=Pr=2, Sr=0.6 $\sigma=1,\phi=\pi/4$,M=4 and $dp/dx=1$.

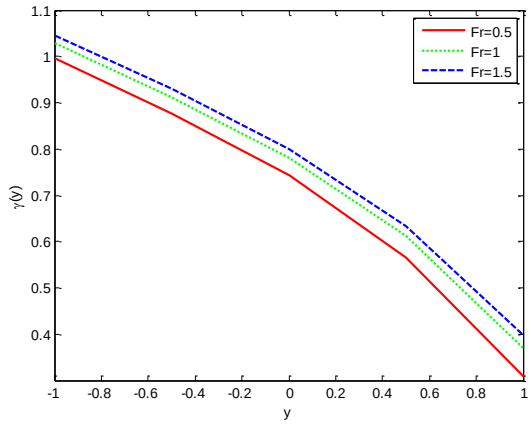

Figure 19. Plot of temperature profile $\gamma(y)$ for various values of Fr with $a=0.6$, b=0.7, d=1.5, R=0.5, $\eta=0.1$,m=0.03, $\theta=\pi/3$, x=-0.5, Du=0.1, Sc=0.5,Br=Pr=2, Sr=0.6 $\sigma=1,\phi=\pi/4$,M=4 and $dp/dx=1.$

3.4 Concentration profile.

Here we plot the figures between the concentration profile $\varphi(y)$and several values of physical parameters and determines the performance of concentration profile $\varphi(y)$. As per Figure 20, $\varphi(y)$is directly proportional to η. In couple stress fluid $(\eta\neq 0)$ the concentration profile $\varphi(y)$ is strengthened when compared to couple stress fluids $(\eta\to 0)$. Figure21 reveals that $\varphi(y)$ increases with the increase of Hartmann number M due to decrease of the velocity. Figure 22 depicts, "for subcritical flow $(Fr<1)$ the concentration profile $\varphi(y)$ higher when compared to the critical (Fr=1) and supercritical (Fr>1) flows which says that the Froude number Fr is opposite phenomenon of the concentration profile $\varphi(y)$".Figure 23 show that the $\varphi(y)$decreases with the increases of Hall parameter m.

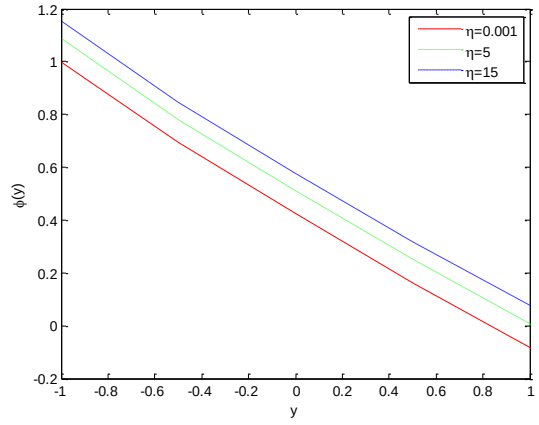

Figure 20. Plot of temperature profile $\varphi(y)$ for various values of η with $a=0.6$, b=0.7, d=1.5, R=0.2, M=2, Fr=1.2, m=0.03, x=-0.5, Du=0.1, Sc=1, Br=2, Pr=4, Sr=0.6 $\sigma=1,\phi=\pi/4,\theta=\pi/3$ and $dp/dx=2$.

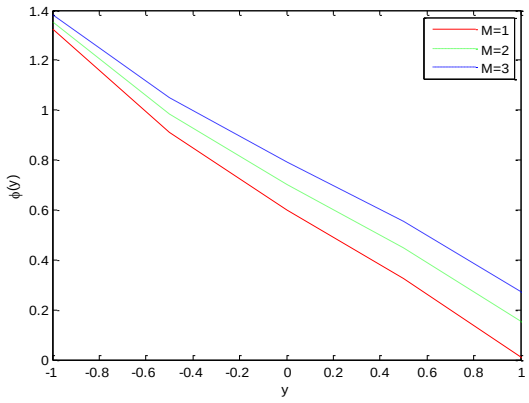

Figure 21. Plot of temperature profile $\varphi(y)$ for various values of M with $a=0.6$, b=0.7, d=1.5, R=0.2, $\eta=0.1$, Fr=1.2, m=0.03, x=-0.5, Du=0.1, Sc=1, Br=2, Pr=4, Sr=0.6 $\sigma=1, \phi=\pi/4$, $\theta=\pi/3$ and $dp/dx=2$.

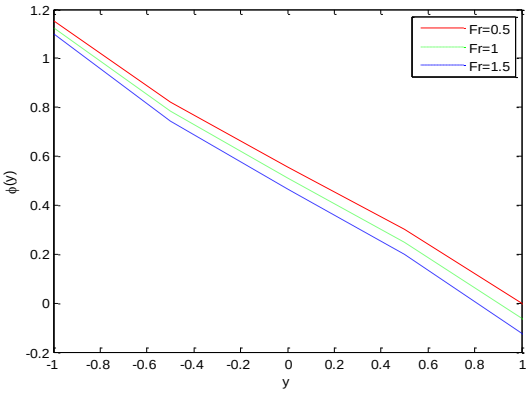

Figure 22. Plot of temperature profile $\varphi(y)$ for various values of Fr with $a=0.6$, b=0.7, d=1.5, R=0.2, M=2, $\eta=0.1$, m=0.03, x=-0.5, Du=0.1, Sc=1, Br=2, Pr=4, Sr=0.6 $\sigma=1, \phi=\pi/4, \theta=\pi/3$ and $dp/dx=2$.

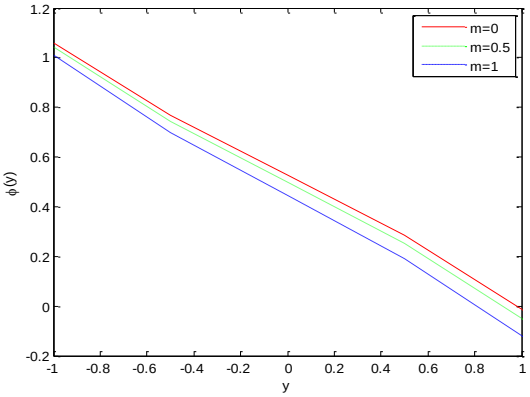

Figure 23. Plot of temperature profile $\varphi(y)$ for various values of m with $a=0.6$, b=0.7, d=1.5, R=0.2, M=2, $\eta=0.1$, Fr=1.2, x=-0.5, Du=0.1, Sc=1, Br=2, Pr=4, Sr=0.6 $\sigma=1, \phi=\pi/4, \theta=\pi/3$ and $dp/dx=2$.

4. Conclusions

The impact of Hall effect on peristaltic flow of couple stress fluid in a vertical asymmetric channel with heat and mass transfer is studied. The outcomes are discussed by plotting diagrams and are given below.

- The couple stress parameter η increases where as pressure gradient increases in the narrow part and decreases in wider part of the channel.
- The behavior of Hall parameter m is inversely proportional couple stress parameter η on dp/dx.
- With the increase of Hall parameter m, the pressure rise Δp_λ increase in the copumping region and decrease in the retrograde region.
- Pressure rise Δp_λ decreases in all pumping regions with the Froude number Fr increases.
- The velocity profile $u(y)$ increases with the increase of Froude number Fr and Hall parameter m, and it is decreases with the increases of couple stress parameter η and Hartmann number M.
- The temperature profile $\gamma(y)$ is directly proportional to sevaral values of Hall parameter m and Froude number Fr and it is inversely proportional to couple stress parameter η and Hartmann number M.
- Concentration Profile $\varphi(y)$ is inversely proportional to function of Fr and m and $\varphi(y)$ is directly proportional to η and M

References

[1] Latham T W 1996 *M.sc. thesis*, MIT, Cambridge, MA
[2] Shapiro A H, Jaffrin M Y and Weinberg S L 1969 *J. Fluid Mech.* **37** 799-825
[3] Abdelmaboud Y 2012 Nonlinear *Sci. Numer. Simulat*. **17** 685-698
[4] Akram S and Nadeem S 2013Closed from solutions, *J.Magn. Mater* **328** 11-20
[5] Hari Prabakaran P, Hemadri Reddy R, Saravana R, Kavitha A and Sreenadh S 2015 *Advances and Applications in Fluid Mechanics*,**17(1)** 1-16
[6] Saravana R, Sreekanth S, Sreenadh S, Hemadri Reddy R, 2011 *Advances in Applied Science Research*, **2(1**) 221-229
[7] Vajravelu K, Sreenadh S, Saravana R, 2013 *Applied Mathematics and Computation,* **225** 656-676
[8] Hameed M and Ellahi R 2011 *Int. J. Numer. Meth. Fluids* **67** 1234- 1246
[9] Mekheimer Kh S, Salem A M and Zaher A Z 2014 *J. Egyptian Math. Soc*. **22** 143-151
[10] Hari Prabakaran P, Hemadri Reddy R, Sreenadh S, Saravana R, and Kavitha A, 2012 *Int. J. Applied Mathematics and Mechanics* **8(13)** 68- 83
[11] Srinivas S, Gayathri R and Kothandapani M 2011 *Commun Nonlinear Sci. Numer. Simulat*. **16** 1845-1862
[12] Saravana R, Sreenadh S, Venkataramana S, Hemadri Reddy R, Kavitha A 2011 *I J I T&E***, 1(11)** 10-24
[13] Seeshan A and Ellahi R 2013 *Appl. Math. Inf. Sci*. **7** 257-265
[14] Stokes V K 1996 *Phys. Fluids* **9** 1709-1715
[15] Cowin S C 1974 *Adv. Appl. Mech*. **14** 279-347
[16] Beg O A, Zueco J and Chang T B 2011 *Chem. Engrg. Common*. **198** 312-331
[17] Ali N and Hayat T 2008 *Comput. Math. Appl*. **55** 589-608
[18] Hayat T, Ali N and Asghar S 2007 *Phys. Lett. A* **363** 397-403

[19] Srinivas S and Gayathri R 2009*Applied Mathematics and Computation* **215** 185–196
[20] Nadeem S and Akbar N S 2011 *Journal of the Taiwan Institute of Chemical Engineers***, 42(1)** 58–66
[21] Kavitha A, Hemadri Reddy R, Sreenadh S, Saravana R and Srinivas A N S 2011 Pelagia Research Library, *Advances in Applied Science Research* **2**(1) 269-279
[22] Vajravelu K, Sreenadh S and Lakshminarayana P 2011 **16** 3107–3125
[23] Rami Reddy G and Venkataramana S 2011 Pelagia Research Library, *Advances in Applied Science Research* **2**(5) 240-248
[24] Gad N S 2011 *Appl.Math. Comput*. **217** 4313-4320
[25] Abo-Eldahab E, Barakart E and Nowar Kh 2012 *Math. Probl. Engrg*. 840203
[26] Hayat T, Maryam Iqbal, Humaira Yasmin and Faud Alsaadi 2014 *Int. J. Biomath*. **7(**5) 1450057